



## Hydrothermal synthesis and electrochemical performance of energy storage material and its photocatalytic activity of Fe<sub>2</sub>O<sub>3</sub>/ pyrrole composite

Dr.J.Johnny Caroline<sup>1</sup>,Karthiga .D<sup>2</sup>

<sup>1</sup>Assistant professor, Department of Chemistry,Nirmala college forwomen,Coimbatore, Tamil Nadu, India

<sup>2</sup>Department of Chemistry, Nirmala college for women, Coimbatore, Tamil Nadu, India

email I'd: [1johnnyever@gmail.com](mailto:1johnnyever@gmail.com)<sup>2</sup>[karthigadhanaraj@gmail.com](mailto:karthigadhanaraj@gmail.com)

### Article History

Volume 6, Issue 8, 2024

Received: 16 May 2024

Accepted: 28 June 2024

Doi:

10.48047/AFJBS.6.8.2024.3179-3185

### Abstract

The pyrrole, Fe<sub>2</sub>O<sub>3</sub>, and Fe<sub>2</sub>O<sub>3</sub>/Pyrrole composites was synthesized by a simple hydrothermal method. The morphological characterizations (FE-SEM) indicated the Fe<sub>2</sub>O<sub>3</sub>covered by Pyrrolenanosheets. Optical features of the synthesized samples were examined by XRD, FTIR, and SEM The catalytic efficacy of methylene blue dye degradation is 93.4 % in 100 min, it is higher than that of pristine Pyrrole(40%) and Fe<sub>2</sub>O<sub>3</sub> (72%). Fe<sub>2</sub>O<sub>3</sub>/PPy composite shows outstanding catalytic steadiness and efficiency, it still maintains the catalytic efficiency. The catalytic enhancement due to the high specific surface area of Pyrrole, and also the composite shows high reliability and degradation efficiency. Theprepared material is a potential candidate for high performance energy storage and photocatalytic applications

**Keywords:** Fe<sub>2</sub>O<sub>3</sub>/Pyrrole, Hybrid, Methylene blue decomposition, Catalytic mechanism.

## INTRODUCTION

Due to the growing globalization and urbanization, eco-logical adulteration and energy crisis was crucial issue, and thus seeking sustainable and renewable energy sources. Water is the main resource, not only for humans, water is necessary for all living organisms in these worlds, but nowadays wastewater effluence is a major issue. These pollutants are degrading a river, sea, lakes, and other water resources, this contamination reduces the water quality and causes a probable menace to living organisms and environmental systems for a long-time duration. So, the purification of textile industry wastewater (particularly dye components) is a necessity for a green and clean environment. Currently, various techniques are used for wastewater purification such as reverse osmosis, photo-electrochemical water-splitting, sonocatalysis, photocatalysis, ion-exchange, and membrane filtration, among these techniques photocatalysis, offers excessive aid to contract with the ecological tasks and sustainability with solar-light.

In this situation, photocatalysis is a fast-growing field. The advantages of using active photocatalysts are fully mineralizing the organic pollutants into H<sub>2</sub>O and CO<sub>2</sub> without any toxic

intermediate. Semiconductor metal oxides and sulfides are mostly studied in photocatalytic materials such as ZnO, CuO, Fe<sub>2</sub>O<sub>3</sub>, TiO<sub>2</sub>, WO<sub>3</sub>, NiO, NiS, ZnS, CdS, etc. Titanium oxide is one of the widely studied materials apart from these zinc oxides extensively applied for mineralization of organic pollutants. The pristine metal oxides catalytic efficacy is low due to its higher recombination rate and lower-quantum efficacy affects the practical applications of metal oxides. So, the researchers used some strategies to enhance the efficiency which is doping with some other additives or compositing with additional semiconductor materials.

In this work, we synthesize different Fe<sub>2</sub>O<sub>3</sub>/PPy composites by hydrothermal method followed by chemical oxidation. The optical, functional, morphological, and structural properties of prepared materials were studied by FTIR, XRD, and SEM. The dye degradation efficacy of the synthesized samples was examined against methyl orange under the irradiation of a halogen lamp and the probable degradation mechanism of the synthesized materials has been proposed.[1].

## **METHODOLOGY**

### **2.1 Materials**

Ferric Chloride hexahydrate (Sigma Aldrich), Pyrrole (Py, A.R.), and sulfuric acid (98 wt%) were procured from Sisco Research Laboratories Pvt. Ltd. (SRL) in India. Cetyltrimethyl ammonium bromide, CTAB (98% Merck, India), and ethanol (>99% pure) were also supplied by SRL. All other chemicals were of analytical grade and employed without additional purification. Double-distilled water (DI water) was utilized consistently throughout the study.

### **2.2 Experimental**

#### **2.2.1 Synthesis of Pyrrole**

The synthesis of Pyrrole was carried out by using chemical oxidation method. 1 M of pyrrole monomer is added into 0.5 M HCl solution. In another container, 0.4 M FeCl<sub>3</sub> was prepared. The FeCl<sub>3</sub> solution was then added into the pyrrole monomer at a temperature of nearly 0°C. The pyrrole solution turned black in color, indicating the initiation of polymerization. After 5 hours, the Pyrrole obtained was washed with distilled water and dried overnight at 80°C. The final product was well-grained and stored for further analysis.

#### **2.2.2 Synthesis of Fe<sub>2</sub>O<sub>3</sub>**

Fe<sub>2</sub>O<sub>3</sub> nanomaterials was prepared by a simple hydrothermal method, iron chloride (0.2 M) and (0.2 M) of cetyltrimethyl ammonium bromide were added into 15 ml deionized water under for 30-minutes magnetic stirring at room temperature. The resultant solution was transferred into a 50 ml Teflon-lined stainless autoclave and heated for 12 hours at 180°C in a hot air oven, then it was allowed to cool at room temperature. The precipitate was centrifugated, washed with excess distilled water and ethanol, and finally dried at 60°C to obtain Fe<sub>2</sub>O<sub>3</sub>.

#### **2.2.3 Synthesis of Fe<sub>2</sub>O<sub>3</sub> at Pyrrole**

The pyrrole monomer is chemically oxidized with synthesized iron oxide nanoparticles to create Fe<sub>2</sub>O<sub>3</sub> at Pyrrole composite.

## **Results and Discussion**

### **3.1 Characterization Techniques**

#### **3.1.1 X-ray Powder Diffraction (XRD)**

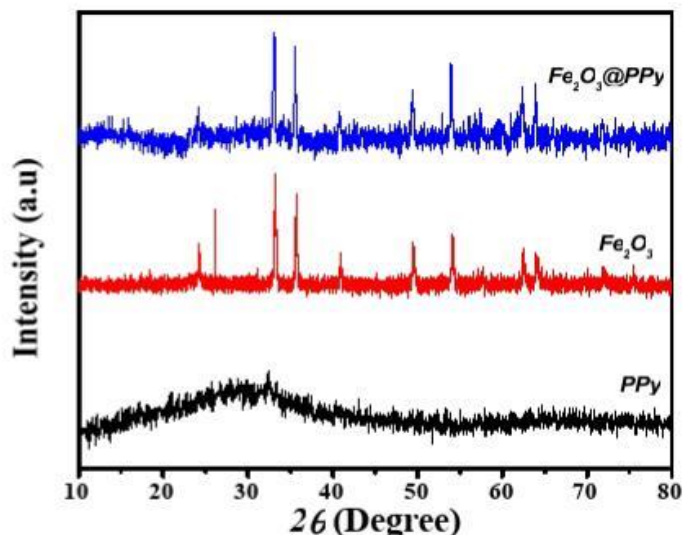


**Fig. 1 XRD Pattern of a) pyrrole, and b)  $\text{Fe}_2\text{O}_3$ , c)  $\text{Fe}_2\text{O}_3$  at pyrrole**

To examine the crystallinity and crystal phases, the as-synthesized iron oxide nanoparticles were examined by X-ray diffraction (XRD). Fig. 1 exhibits the typical XRD pattern of as-synthesized nanoparticles and composites. Several well-defined diffraction reflections are seen in the observed. pyrrole shows a broad peak at  $26.4^\circ$  which denotes that the synthesized polypyrrole is amorphous in nature, XRD patterns is well matched with the rhombohedral  $\alpha\text{-Fe}_2\text{O}_3$  structures with calculated lattice constants of  $a = 5.0356 \text{ \AA}$  and  $c = 13.7489 \text{ \AA}$ . The observed XRD pattern is well matched with the reported literature and JCPDS No  $\sim 33\text{-}0664.25$  Except for rhombohedral  $\alpha\text{-Fe}_2\text{O}_3$ , no reflection for other impurities was found in the pattern which reveals that the prepared nanoparticles are pure  $\alpha\text{-Fe}_2\text{O}_3$ . In addition to this, due to sharp and strong diffraction reflection, one can confirm that as-synthesized nanoparticles are well-crystalline.  $\alpha\text{-Fe}_2\text{O}_3$  at pyrrole shows almost same peaks with the amorphous peak which indicates that the iron oxide is well adopted to the polymer matrix.

### 3.1.2 Fourier-transform infrared spectroscopy (FTIR)

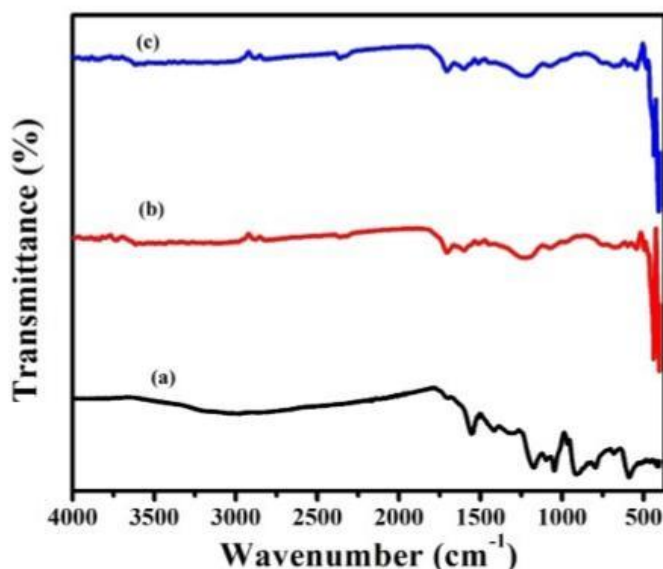


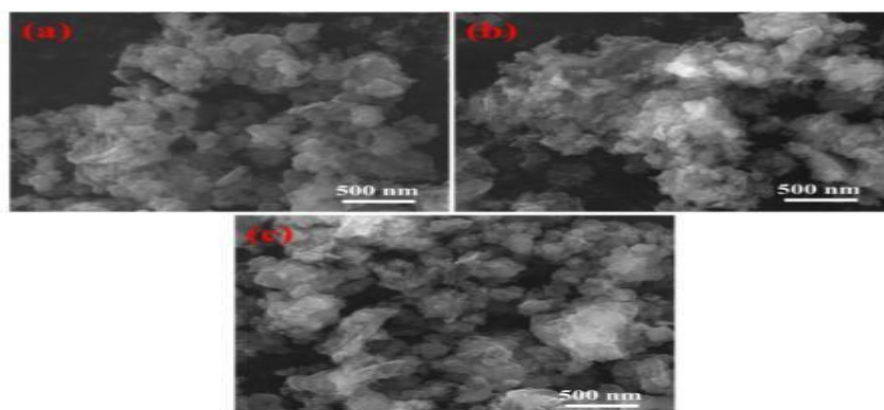
**Fig. 2 FTIR spectrum of a) Pyrrole, b) Fe<sub>2</sub>O<sub>3</sub>, and c) Fe<sub>2</sub>O<sub>3</sub> at Pyrrole**

The synthesized compounds' FT-IR spectra are displayed in Fig. 9. While the sharp peak at 810 cm<sup>-1</sup> is attributed to the bending vibration of heptazine rings, indicating that the synthesized Pyrrole is composed of heptazine units, the broad absorption band around 3200 cm<sup>-1</sup> originates from the stretching vibration of the N-H bond, which is associated with uncondensed amino groups of Pyrrole. The peak at 1718 cm<sup>-1</sup> is associated with C=O group. 1534 is attributed to the C=C functionality of the polymer matrix [2]. 780 cm<sup>-1</sup> associated to the out-plane bending vibration of peaks of Pyrrole. Iron oxide shows a broad peak at 3500 cm<sup>-1</sup> associated with the hydroxyl group, and a peak at 450 cm<sup>-1</sup> is associated with the metal-oxygen bond (M-O) The characteristic do not move in Fe<sub>2</sub>O<sub>3</sub>/ pyrrole curves, exist in the Fe<sub>2</sub>O<sub>3</sub>/ Pyrrole composite, and the characteristic peaks of Pyrrole are not affected by the structural features of Pyrrole. For comparison, [3]. These peaks are well matched with the Fe<sub>2</sub>O<sub>3</sub>/ Pyrrole composite which indicates that the Iron oxide and graphitic carbon nitride matrix are chemically bonded together in the Fe<sub>2</sub>O<sub>3</sub>/ Pyrrole composite [4]

### 3.1.3 Scanning electron microscopy (SEM) analysis

**Fig. 3 SEM images of a) Pyrrole, a) Fe<sub>2</sub>O<sub>3</sub>, and c) Fe<sub>2</sub>O<sub>3</sub> at Pyrrole**

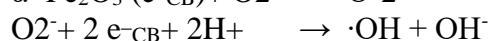
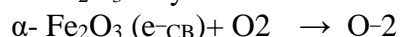
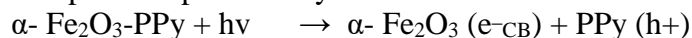
The SEM images of the synthesized samples were shown in fig 3. The synthesized Pyrrole, nanoparticle SEM images are displayed in Fig 10(a) the particles not show well preferable shapes they look like a flake and rock-like morphologies and Fe<sub>2</sub>O<sub>3</sub> shows a slightly flake-like structure and the Fe<sub>2</sub>O<sub>3</sub> and Pyrrole composites shows the aggregated texture with Pyrrole . The aggregated particles had a size of 100 – 150 nm and appeared as flake crystals. The nonobvious difference was observed in surface morphologies in Fe<sub>2</sub>O<sub>3</sub> and Pyrrole samples. This may imply that surfactant molecules are distributed homogeneously into the micropores of Fe<sub>2</sub>O<sub>3</sub>atPyrrole samples [5-6].



### 3.1.4 Application studies of Photocatalytic Activity

The photocatalytic activity of Fe<sub>2</sub>O<sub>3</sub>,pyrrole, and Fe<sub>2</sub>O<sub>3</sub> at Pyrrole composite was examined by the degradation of an aqueous methylene blue solution as a model dye (10mg / L), irradiated under 500W Halogen lamp illumination kept at a distance of 15 cm from the photoreactor Fig.4 revealed the dye degradation mechanism. For typical photocatalytic activity, a minimum amount of 50 mg synthesized nanoparticles is added to the 100 mL aqueous solution of methylene blue with an initial concentration of 10 mg/L under ambient conditions and are allowed to continue stirring for 1 hour under the dark condition to achieve an equilibrium of adsorption-desorption. A xenon lamp then exposed the mixture to begin the photocatalytic process. 5 mL of solution was pipetted out at regular intervals of 20 min. The concentration of dye molecules in the collected sample was measured from the absorbance spectra recorded on JASCO V-670 double beam spectrophotometer.

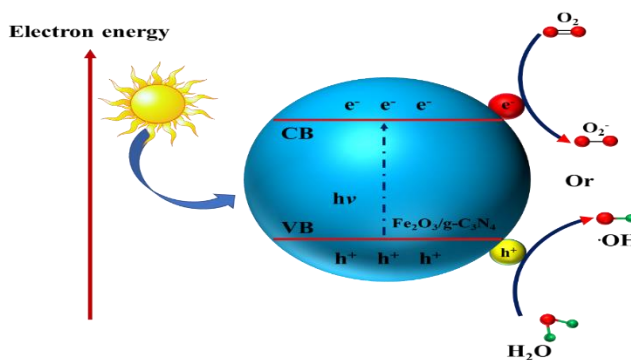
The possible photocatalytic reactions are similar to those reported In the literature as follows [7]



MB + ·OH → oxidation products (CO<sub>2</sub>, H<sub>2</sub>O etc) The photocatalytic degradation efficiency of dyes was calculated in the following equation .

$$D = \frac{(A_0 - A)}{A_0} \times 100\% \dots\dots\dots (4.1)$$

Whereas is the initial concentration of dye and A is the concentration of dye after photoirradiation.



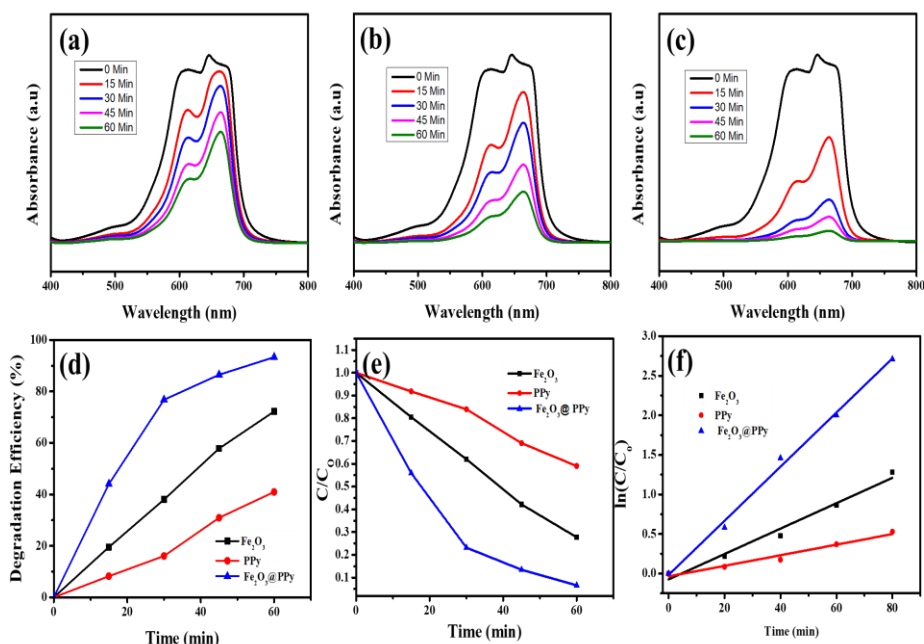


**Fig. 4 Photocatalytic activity of a) Fe<sub>2</sub>O<sub>3</sub>, b) Pyrrole, C) Fe<sub>2</sub>O<sub>3</sub>@Pyrrole, d,e) degradation efficacy. F) First-order kinetics plot for the photodegradation of MB**

The photocatalytic behavior of Fe<sub>2</sub>O<sub>3</sub>, pyrrole at Fe<sub>2</sub>O<sub>3</sub> and Pyrrole nanoparticles was carried out under UV-light irradiation was analyzed using methylene blue degradation and the results are as shown in Fig. 12 (a,b,c). First of all, under UV light irradiation, a blank experiment without any photocatalyst was conducted to verify the ability of photocatalysis of semiconductor nanoparticles. The analyzed results showed that the synthesized Fe<sub>2</sub>O<sub>3</sub>, pyrrole, and Fe<sub>2</sub>O<sub>3</sub>@Pyrrole nanoparticles were degraded by the methylene blue dye is 72%, 40.5% and 93.4% in 60 min. from these results, we conclude the Fe<sub>2</sub>O<sub>3</sub>@ pyrrole composite is a promising catalyst for methylene blue dye degradation. It is evident from fig.12 (d,e). that the photocatalytic activity of Fe<sub>2</sub>O<sub>3</sub>@ pyrrole is higher than that of pristine Fe<sub>2</sub>O<sub>3</sub> at pyrrole nanoparticles. It showed the degradation efficacy of 93.4% in 60 min. This is due to the synergetic effect between the pristine Fe<sub>2</sub>O<sub>3</sub>, atpyrrole nanoparticles it enhances the specific surface areas of the Fe<sub>2</sub>O<sub>3</sub>@ pyrrole composite. Surface area and crystallinity play a key role in the catalyst's photocatalytic function. Nevertheless, it has been found in the present case that crystallinity and surface area play an important role in photocatalytic activity rather than the particular region of the substance. The crystallinity and surface area make the formation of hydroxyl radicals more transparent polar faces, which are responsible for the degradation of dye molecules [8].

As can be seen from Fig. 4 (e), the photodegradation of MB by Fe<sub>2</sub>O<sub>3</sub>, pyrrole, Fe<sub>2</sub>O<sub>3</sub>@ pyrrole composite followed a first-order rate law,

$$\ln(C_t/C_0) = -kt$$

Where C<sub>0</sub> is initial concentration of methylene blue (mg/l). C<sub>t</sub> is the concentration of the dye at various interval times (mg/l), t is the illumination time (min) and k is the reaction rate constant.

## CONCLUSION

Herein the Fe<sub>2</sub>O<sub>3</sub>, pyrrole at Fe<sub>2</sub>O<sub>3</sub> at pyrrole composite synthesis via one-pot hydrothermal method. The structural, morphological, and optical features of the synthesized samples were examined by XRD, FTIR, and SEM. Fe<sub>2</sub>O<sub>3</sub> at pyrrole shows the catalytic efficacy of methylene blue dye degradation is 93.4 % in 60 min, it is higher than that of pure Fe<sub>2</sub>O<sub>3</sub> at Pyrrole. Fe<sub>2</sub>O<sub>3</sub> at

pyrrole composite shows outstanding catalytic steadiness and efficiency, it still maintains the catalytic efficiency. These results propose the Fe<sub>2</sub>O<sub>3</sub>at pyrrole composite is a promising material for high-performance energy storage and photocatalytic application.

#### REFERENCE

1. Julie Ann Joseph, Sinitha B. Nair, Sareen Sarah John, Stephen K. Remillard, SadasivanShaji, Rachel Reena Philip1 Journal of Applied Electrochemistry (2021).  
<https://doi.org/10.1007/s10800-020-01512-2>
2. Muhammad AzamQamar, SammiaShahid, MohsinJaved, Shahid Iqbal, Mudassar Sher, Ali Bahadur, MurefahMana AL-Anazy, A. Laref, Dongxiang Li. Designing of highly active g-C<sub>3</sub>N<sub>4</sub>/Ni-ZnO photocatalyst nanocomposite for the disinfection and degradation of the organic dye under sunlight radiations. Colloids and Surfaces A: Physicochemical and Engineering Aspects (2021).  
<https://doi.org/10.1016/j.colsurfa.2021.126176>
3. M. Faisal, Md A. Rashed, Jahir Ahmed, MabkhootAlsaieri, Mohammed Jalalah, S. A. Alsareii, Farid A. Harraz. Au nanoparticles decorated polypyrrole-carbon black/g-C<sub>3</sub>N<sub>4</sub> nanocomposite as ultrafast and efficient visible light photocatalyst. Chemosphere (2022).  
<https://doi.org/10.1016/j.chemosphere.2021.131984>
4. Xiaoqian Wei, Xin Wang, Yu Pu, Annai Liu, Chong Chen, Weixin Zou, Yulin Zheng, Jinsheng Huang, Yue Zhang, Yicheng Yang, Mu. Naushad, Bin Gao, Lin Dong. Facile ball-milling synthesis of CeO<sub>2</sub>/g-C<sub>3</sub>N<sub>4</sub> Z-scheme heterojunction for synergistic adsorption and photodegradation of methylene blue: Characteristics, kinetics, models, and mechanisms. Chemical Engineering Journal (2020).  
<https://doi.org/10.1016/j.cej.2020.127719>
5. Guang Fan, Zhanying Ma, Xiaobo Li, Lingjuan Deng. Coupling of Bi<sub>2</sub>O<sub>3</sub> nanoparticles with g-C<sub>3</sub>N<sub>4</sub> for enhanced photocatalytic degradation of methylene blue. Ceramics International (2020).  
<https://doi.org/10.1016/j.ceramint.2020.10.162>
6. FeiChanga, YunchaoXiea, Chenlu Li, Juan Chena, JieruLuo, Xuefeng Hu, Jiaowen Shen. A facile modification of g-C<sub>3</sub>N<sub>4</sub> with enhanced photocatalytic activity for degradation of methylene blue. Applied Surface Science (2013).  
<http://dx.doi.org/10.1016/j.apsusc.2013.05.127>
7. Shengqiang Zhang, Changsheng Su, Hang Ren, Mengli Li, Longfeng Zhu, Shuang Ge, Min Wang, Zulei Zhang, Lei Li, and Xuebo Cao. In-Situ Fabrication of g-C<sub>3</sub>N<sub>4</sub>/ZnO Nanocomposites for Photocatalytic Degradation of Methylene Blue: Synthesis Procedure Does Matter. Journal of Nanomaterials (2019).  
<http://dx.doi:10.3390/nano9020215>
8. YingchangKe, HongxuGuo, Dongfang Wang, Jianhua Chen, and Wen Weng. YingchangKe, HongxuGuo,a) Dongfang Wang, Jianhua Chen, and Wen Weng. Journal of Materials Research (2014).  
<http://dx.doi:10.1557/jmr.2014.276>